ACS APPLIED MATERIALS & INTERFACES

RESEARCH ARTICLE

www.acsami.org

Synthesis and Characterization of Silica Nanoparticles with Well-Defined Thermoresponsive PNIPAM via a Combination of RAFT and Click Chemistry

Jiucun Chen, Mingzhu Liu,* Chen Chen, Honghong Gong, and Chunmei Gao

State Key Laboratory of Applied Organic Chemistry, Key Laboratory of Nonferrous Metal Chemistry and Resources Utilization of Gansu Province and Department of Chemistry, Lanzhou University, Lanzhou 730000, People's Republic of China

ABSTRACT: Covalent functionalization of azide-modified SiO_2 with well-defined, alkyne-terminated poly(N-isopropylacrylamide) was accomplished by the Cu(I)-catalyzed [3 + 2] Huisgen cycloaddition. The alkyne-terminated RAFT chain transfer agent was first synthesized, and then the alkyne-terminated thermoresponsive poly(*N*-isopropylacrylamide) (PNIPAM) with different molecular weights were synthesized by the RAFT of NIPAM monomer. The polymerization kinetics and the evolution of number-average molecular weights (M_n), and polydispersities (M_w/M_n), with monomer conversions were investigated. A copper(I)-catalyzed azide−alkyne cycloaddition (CuAAC) "grafting to" method was used to attach thermoresponsive polymers onto the exterior surface of SiO_2 nanoparticles which produced relatively high grafting density. The as-synthesized hybrid nanoparticles showed thermoresponsive behavior and were characterized by FTIR, XPS, TGA, DLS, and TEM, etc.

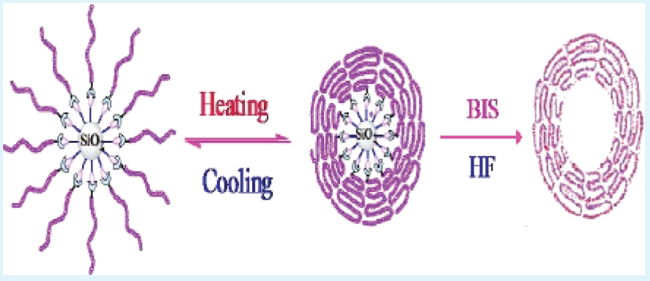

KEYWORDS: RAFT polymerization, click chemistry, surface modification, thermoresponsive

1. INTRODUCTION

The polymer/inorganic nanocomposites have gained great attention in recent years as their excellent properties, such as mechanical properties, thermal stability and flame retardance, gas barrier properties, biodegradation, and abrasion resistance.[1−4] The inorganic particles' surface modification is a kind of typical method to prepare polymer/inorganic hybrid materials. There are two ways to attach the polymer chains to the surface of inorganic particles: "grafting to"[5] and "grafting from"[6−8] techniques. Although the "grafting from" approach promises high graft density, attachment of initiator groups to inorganic surfaces and control over polymer molecular weight and architecture can be difficult to achieve. Additionally, the widely used controlled radical polymerizations that have been reported to occur from inorganic surfaces may be affected by radical coupling to substrates, potentially causing side reactions can reduce the controllability of the polymerization process. Conversely, "Grafting to" approach refers to preformed, end-functionalized polymers reacting with a suitable substrate surface under appropriate conditions to form a tethered polymer brush. The covalent bond formed between surface and polymer chain makes the polymer brushes robust and resistant to common chemical environmental conditions. This method has been used often in the preparation of polymer brushes. End-functionalized polymers with a narrow molecular weight distribution can be synthesized by living anionic, cationic, radical, group transfer and ring-opening metathesis polymerizations. The substrate surface also can be modified to introduce suitable functional groups by coupling agents or SAMs. In addition, most of the reported inorganic surfaces grafting reactions require relatively harsh conditions, typically involving high-temperature and long reaction time. Such conditions may be incompatible with many of the functional molecules that are desirable for grafting onto substrates.[9,10]

Therefore, there is a strong driving force to explore new robust and efficient grafting approaches to tailor the properties of inorganic materials. One potential method for achieving high graft density while maintaining control over the polymer structure involves the application of a modular approach where substrates bearing a controllable number of highly reactive surface species are coupled to separately prepared, end-functionalized polymers using an efficient (preferably quantitative) coupling protocol. Recently, the Cu(I)-catalyzed [3 + 2]-cycloaddition reactions between an azide and an alkyne, i.e., "click reactions", as termed by Sharpless and co-workers,[11] have gained a great deal of attention because of their high specificity and nearly quantitative yields in the presence of many functional groups. Because of its quantitative yield, mild reaction conditions, and tolerance of a wide range of functional groups, Cu(I)-catalyzed azide−alkyne cycloadditions (CuAACs) have been shown to be an almost universal tool for modifying polymers, dendrimers, rotaxanes, inorganic surfaces, colloidal nanoparticles, and even biological entities such as cells, viruses, or proteins.[12−18]

Received: June 3, 2011
Accepted: July 27, 2011
Published: July 27, 2011

dx.doi.org/10.1021/am2007189 | *ACS Appl. Mater. Interfaces* 2011, 3, 3215–3223

Hence, most drawbacks of standard "grafting to" approaches have been offset by the strong efficiency of the CuAAC process.

The combination of living/control radical polymerization and click reaction has been a powerful strategy in the preparation of functional hybrid materials.[19,20] Among the available living/control radical polymerization (CRP) techniques, the reversible addition−fragmentation transfer (RAFT) polymerization has been proven to be one of the more versatile CRP techniques allowing the controlled polymerization of a wide variety of monomers under mild reaction conditions.[21] In principle, the polymers obtained by RAFT polymerization are end-capped by the moieties derived from the RAFT agent. As a result, the functional groups can be easily introduced into the chain ends of the polymers, by adjusting the structure of the RAFT agent used in RAFT process.[22,23] On the other hand, in contrast to the large number of reports using ATRP to prepare polymer grafted substrates, there are surprisingly few reports on the application of RAFT techniques to the synthesis of polymer grafted substrates, probably because of the difficulty in covalently attaching RAFT agent to a substrate.[24]

Functional polymers are ideal building blocks for nanofabrication and engineering of surfaces because of their response in shape and size to environmental changes. It is an attractive idea to functionalize nanoparticles with stimuli-responsive polymers, and the obtained materials can be used to control the release of guest molecules under external stimuli, such as ionic strength, pH, and temperature.[25−28] Perhaps the most extensively studied stimuli-responsive hybrid nanomaterials are those coated with thermoresponsive poly(*N*-isopropylacrylamide) (PNIPAM) brushes. PNIPAM has been well-known as a thermoresponsive polymer, exhibiting a lower critical solution temperature (LCST) at ∼32 °C.[29] We present herein CuAAC-based grafting approaches for the versatile and efficient functionalization of nanoparticles. These approaches are based on tailor-made azide-functionalized nanoparticles and alkyne-functionalized thermosensitive brush precursors. We also extended the possibilities by combining both CRP techniques and click chemistry to improve the complexity and the density of the polymer corona, as shown in previous work on silica nanoparticles in Scheme 1. To the best of our knowledge, this is the first example for the synthesis SiO_2-supported organic/inorganic thermosensitive nanomaterials via RAFT polymerization and click reaction.

Scheme 1. Schematic Illustration of the Synthesis of Hybrid Silica Nanoparticles Coated with Thermoresponsive PNIPAM Brushes via RAFT Polymerization and Click Chemistry

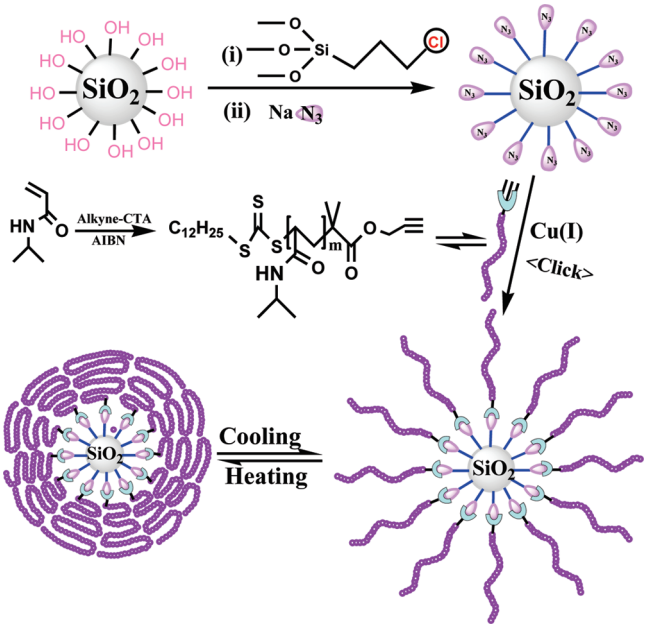

2. EXPERIMENTAL SECTION

2.1. Materials. N-Isopropylacrylamide (NIPAM, 99%) was obtained from Tokyo Kasei Kagyo Co. and recrystallized from *n*-hexane, then dried under a vacuum. Tetrahydrofuran (THF) and 1,4-dioxane were refluxed over sodium and distilled twice before use. Dimethylformamide (DMF) was dried by refluxing over CaH_2 and distilled just before use. The nanosilica with the average diameter of 50 nm was provided by Aladdin Reagent Co. and was kept at 120 °C in vacuum for 36 h prior to use. Sodium azide, N-(3-(dimethylamino)propyl)-N′-ethylcarbodiimide hydrochloride (EDC·HCl), 4-(dimethylamino) pyridine (DMAP), N,N′-methylenebisacrylamide (BIS), propargyl alcohol, and (3-chloropropyl)trimethoxysilane were purchased from Aladdin Reagent Co. with the highest purity and used as received without further purification. Azodiisobutyronitrile (AIBN) was purchased from Aldrich and recrystallized from ethanol. All other reagents were purchased from commercial sources and used as received.

2.2. Instruments and Measurements. FTIR spectroscopy patterns were performed on a Dig lab FTS 3000 instrument. Gel permeation chromatography (GPC) analysis of the samples was performed at a flow rate of 1.0 mL/min and 40 °C in THF by using Waters GPCV2000 equipment. Elemental analysis (EA) of C, N and H was performed on an Elementar vario EL. Thermogravimetric analysis (TGA) was performed under nitrogen atmosphere at a heating rate of 10 °C/min on a Perkin-Elmer instrument TG/DTA 6300. ^{1}H NMR (400 MHz) spectra of the reversible addition−fragmentation technique chain transfer agent (RAFT CTA) and polymers were recorded on a Varian UNITY-plus 400 spectrometer using $CDCl_3$ as the solvents. The morphologies of the polymer grafted silica nanoparticles and the polymeric nanocapsules were characterized with a JEM-1200 EX/S transmission electron microscope (TEM) (JEOL, Tokyo, Japan). They were dispersed in water in an ultrasonic bath for 15 min, and then deposited on a copper grid covered with a perforated carbon film. The optical transmittance of aqueous solutions of hybrid nanoparticles was acquired at a wavelength of 500 nm on a Perkin-Elmer Lamda 35 UV−visible spectrophotometer using a thermostatically controlled cuvette. X-ray photoelectron spectra (XPS) were performed on a PHI-5702 instrument using Mg Kα radiation with pass energy of 29.35 eV. Dynamic light scattering (DLS) measurements were conducted with a Brookhaven Instruments BI-200SM goniometer and a BI-9000AT digital correlator at fixed angle 90°. The light source was Spectra-physics 127 Helium−Neon laser (633 nm, power 35mW). The time correlation functions were analyzed with a Laplace inversion program (CONTIN). The aqueous solution was filtered through Millipore membranes (0.45 μm pore size). At each temperature the sample was kept for 10 min to reach equilibrium.

The surface grafting density δ (number of chains/nm^2) was calculated using the following equation:[17]

$$\delta = \frac{\left(\frac{W_{Org}}{W_{Inorg}}\right)\rho V_{Particle} N_A}{M_{Org} S_{Particle}} \quad (1)$$

Here, W_{Org} is the weight loss percentage corresponding to the decomposition of the organic component, W_{Inorg} is the residual weight

percentage, ρ is the density of bulk SiO_2 (2.4 g/cm^3), $V_{Particle}$ is the volume of SiO_2 nanoparticle calculated from the average diameter of SiO_2 (50 nm), N_A is Avogadro's number, M_{Org} is the molecular weight of the organic component, and $S_{Particle}$ is the surface area of SiO_2 nanoparticle calculated from the average diameter of SiO_2 (50 nm).

The distance between grafting sites D (nm) was calculated using the following equation:[30]

$$D = (4/\delta\pi)^{1/2} \quad (2)$$

2.3. Preparation of Azide-Modified SiO_2 (SiO_2-N_3). Into a 100 mL dried round-bottom flask, 2 g of silica nanoparticles was ultrasound dispersed in 60 mL of DMF for 30 min, and then 1 g of 3-chloropropyltrimethoxysilane was added and ultrasound was allowed to proceed for 2 h. NaN_3 (2.0 g, 30.77 mmol) was then introduced into the flask and the mixture was stirred at 40 °C for another 12 h. After the reaction, azide-modified silica nanoparticles (SiO_2-N_3) were purified by three centrifugation/redispersion cycles in DMF, H_2O, and MeOH, followed by drying in a vacuum oven at 30 °C.

2.4. Preparation of Alkyne-Terminated Chain Transfer Agent (alkyne-CTA). The synthesis of *S*-1-dodecyl-*S*′-(α,α′-dimethyl-α″-acetic acid)trithiocarbonate chain transfer agent (trithiocarbonate CTA) was carried out according to a previously reported method in the literature.[31] In brief, 4.04 g of dodecanethiol (20 mmol), 10 mL of acetone, and 0.26 g of tetrabutyl ammonium bromide (0.8 mmol) were added into a 50 mL flask, and it was bubbled with nitrogen gas for 30 min at 10 °C. After that, 1.68 g of 50 wt % sodium hydroxide (21 mmol) aqueous solution was added slowly below 10 °C. After stirring for another 15 min, a carbon disulfide solution in acetone was added dropwise (CS_2: 1.525 g, 20 mmol; acetone: 2.015 g, 34.5 mmol). Next, the system was stirred for another 15 min, and then 3.565 g of chloroform (30 mmol) and 8 g of 50 wt % sodium hydroxide (100 mmol) were added below 10 °C. The ice bath was removed 30 min later, and the reaction was carried out for 12 h, and then 30 mL of distilled water and 5 mL of hydrochloric acid (6.8 M) were added. After 30 min, the system was distilled under reduced pressure to remove the volatile solvents and there appeared some yellow precipitation, and which was collected by filtration. Then the precipitation was dissolved into 100 mL isopropanol under strong stirring, and the undissolved residue was removed by filtration. After that, the filtrate was distilled under reduced pressure to remove isopropanol, and the residue was recrystallized in hexane and dried in vacuum for 24 h. At the end, 4.4 g of trithiocarbonate CTA was obtained.

Alkyne-terminated *S*-1-dodecyl-*S*′-(α, α′-dimethyl-α″-propargyl acetate) trithiocarbonate was synthesized by esterification of *S*-1-dodecyl-*S*′-(α, α′-dimethyl-α″-acetic acid) trithiocarbonate and propargyl alcohol. *S*-1-dodecyl-*S*′-(α, α′-dimethyl-α″-acetic acid) trithiocarbonate (2 g, 5.5 mmol), EDC·HCl (2.12 g, 11 mmol), and DMAP (0.067 g, 0.55 mmol) were mixed in 20 mL of dry CH_2Cl_2. Propargyl alcohol (0.635 mL, 11 mmol) was added dropwise to the mixture at 0 °C, and the transparent yellow solution was stirred at room temperature for 48 h. After the reaction, the mixture was washed with distilled water for three times. The ester was further purified with silica column chromatography (eluent: a mixture of petroleum ether and ethyl acetate with a volume ratio of 1:1), and *S*-1-dodecyl-*S*′-(α, α′-dimethyl-α″-propargyl acetate) trithiocarbonate was obtained. The yield of the product is about 84%.

2.5. Synthesis of Alkyne-Terminated Poly(N-isopropylacrylamide). Polymerization of NIPAM was conducted at 70 °C under a nitrogen atmosphere, employing alkyne-terminated trithiocarbonate as the reversible addition−fragmentation technique chain transfer agent (RAFT CTA) and AIBN as the primary radical source. A typical RAFT polymerization procedure was as follows. NIPAM (12.7 g, 112 mmol), alkyne-CTA (225 mg, 0.56 mmol), 1,3,5-trioxane (504 mg, 5.60 mmol, internal standard), AIBN (18 mg, 0.11 mmol) and 1,4-dioxane (80 mL) were sealed in a 250 mL vial equipped with a magnetic stir bar. The solution was purged with nitrogen for 40 min, and the reaction vial was placed in a preheated reaction block at 70 °C. The samples were removed periodically by syringe to determine molecular weight and polydispersity index (PDI) by gel permeation chromatography (GPC) and monomer conversion by ^{1}H NMR spectroscopy. The polymerization was quenched by cooling in liquid nitrogen and exposing the solution to air. The solution was concentrated under vacuum, and the polymer was precipitated into cold ether. The polymer was reprecipitated four times from THF/ether and dried under a vacuum at room temperature for 12 h.

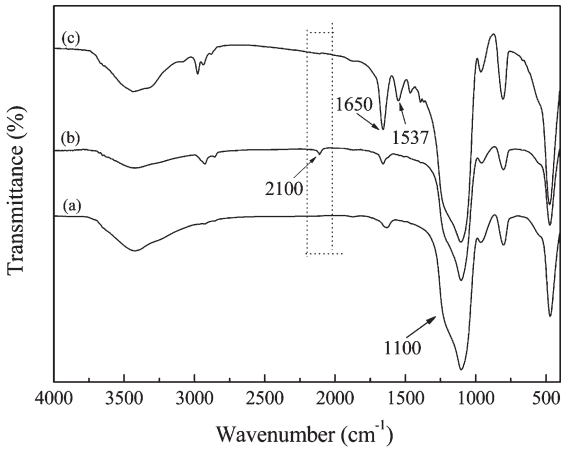

Figure 1. FTIR spectra of (a) bare SiO_2, (b) azide-modified SiO_2, and (c) PNIPAM-functionalized SiO_2.

2.6. Synthesis of the Azide-Modified Silica Nanoparticles with Surface-Clicked PNIPAM Chains via the Alkyne−Azide Click Reaction. 0.200 g of azide modified silica particles and 10.0 mL of DMF were mixed, 1.50 g of alkyne terminated PNIPAM (M_n = 12 200, 0.12 mmol) was added. After ultrasonic treatment for 10 min, a solution of $CuSO_4$ (0.0019 g, 0.012 mmol) in 1 mL of water and another solution of sodium ascorbate (0.0048 g, 0.024 mmol) in 1 mL of water were added orderly into the solution. The reaction was run for 24 h under inert atmosphere at room temperature. After the click reaction, the flask was exposed to air to terminate the polymerization. Nanoparticles were isolated via centrifugation at 10 000 rpm and rinsed with a solution of the sodium salt of EDTA and a water/ethanol (1/1, v/v) mixture (to remove the copper catalyst). Finally, the particles were placed in a Soxhlet extractor and extracted with ethanol for 18 h to remove the unreacted PNIPAM chain, and the obtained PNIPAM-grafted nanoparticles were dried at room temperature in a vacuum oven for 24 h.

2.7. Etching the Silica Templates. AIBN (3 mg) and N,N′-methylenebisacrylamide (12 mg) were added into the suspension of the SiO_2-g-PNIPAM nanoparticles (500 mg) in distilled water (30 mL) and the mixture was stirred at room temperature for 6 h. Then, HF (4 mL, 40%) added to the solution and polymerization was further performed for another 6 h. The solution was dialyzed against deionized water using a dialysis membrane with a molecular weight cut off (MWCO) of 3500 Da for 2 days. Finally, water was removed by freeze-drying.

3. RESULTS AND DISCUSSION

3.1. Analysis of FTIR. FTIR was chosen because the technique is highly sensitive and is able to examine molecules that remain attached to the particle surface.[32] As shown in Figure 1, FTIR spectroscopy provided clear evidence for the step-by-step surface

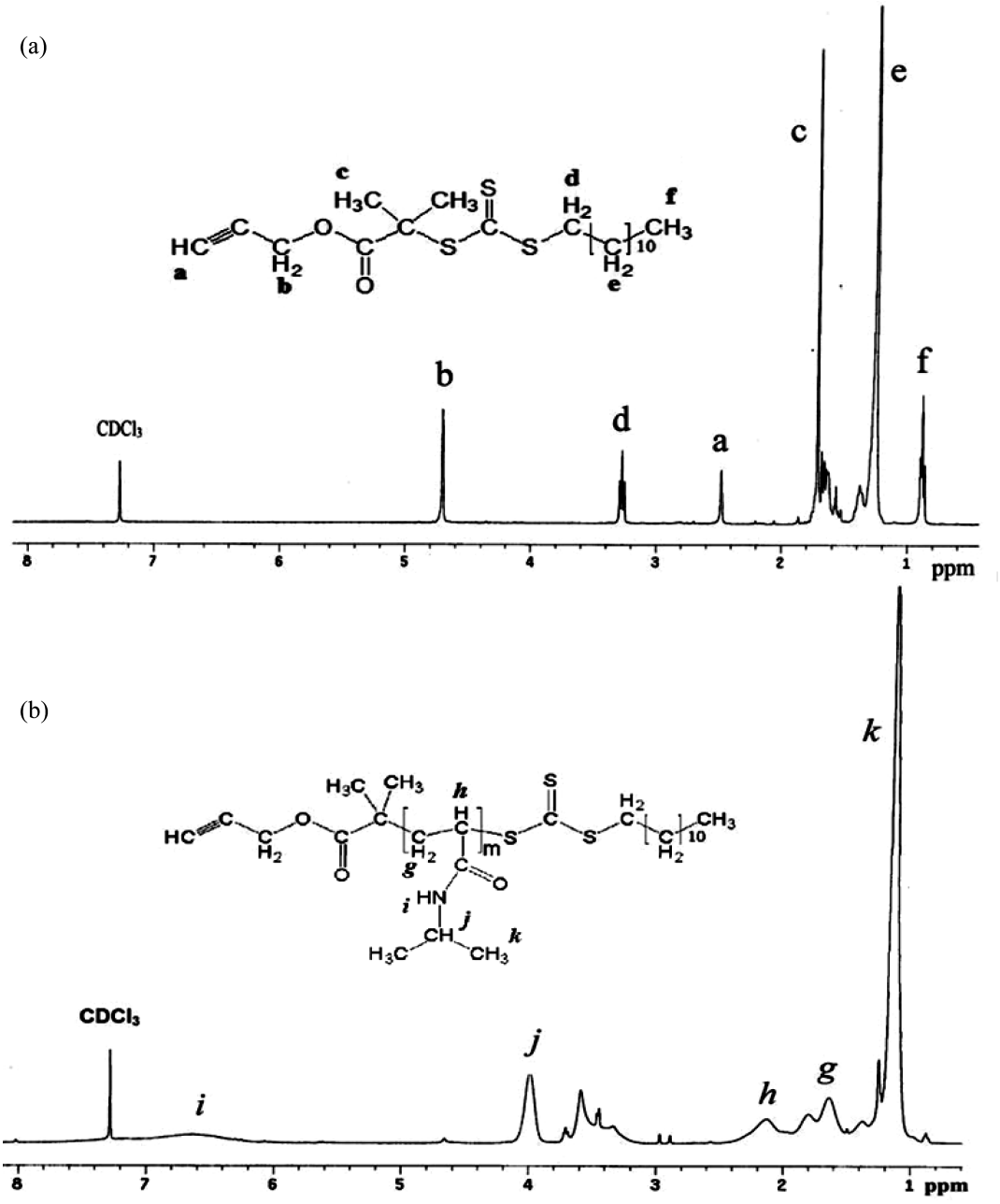

Figure 2. ^{1}H NMR spectra and peak labels for (a) alkyne-CTA and (b) alkyne-PNIPAM. (All measurements were performed in $CDCl_3$ solution, at room temperature, using tetramethylsilane (TMS) as the standard.).

modification. For bare silica nanoparticles (Figure 1a), absorption peaks characteristic of tetrahedron silica structures occur at 1100 cm^{-1} (Si−O stretching) and 465 cm^{-1} (Si−O bending). We can also observe the Si−OH bending at 942 cm^{-1} and the Si−O−Si bending at 800 cm^{-1}. The FTIR spectrum of a typical azide-containing SiO_2 nanoparticle sample is shown in Figure 1b; the sharp absorbance peak at 2100 cm^{-1} corresponds to the -N_3 antisymmetric stretch, whereas the peaks at 2928 and 2858 cm^{-1} correspond to the −C-H stretching and $-CH_2$ stretching vibrations, respectively. This result showed that the silane coupling agent modified SiO_2 nanoparticles were prepared by the self-assembly of 3-chloropropyltrimethoxysilane from the surfaces of SiO_2 nanoparticles and chloride was substituted with an azide group by reaction with sodium azide. Finally, using a click reaction, the azide-modified SiO_2 and alkyne-terminated poly(N-isopropylacrylamide) were reacted to give the corresponding PNIPAM-coated silica nanoparticles in the presence of a $CuSO_4$/Na ascorbate catalyst system in DMF at room temperature. This click reaction was done in the presence of excess polymer. Chidsey and co-workers used quantitative FTIR spectroscopy in their detailed investigation of catalyzed click reaction on gold electrodes.[33] Williams and co-workers recently used FTIR spectroscopy to quantitatively assess the azide/triazole surface coverage on particles over the course of a cycloaddition reaction.[34] As shown in Figure 1c, we can clearly observe the amide I band (1650 cm^{-1}, C═O stretching) and amide II band (1537 cm^{-1}, N−H stretching). The presence of two bands at 1367 and 1388 cm^{-1} are associated with the deformation of two

Table 1. Characterization of Poly(N-isopropylacrylamide) with Alkyne-Functionalized Chain Transfer Agents from RAFT

samples	time (min)	$M_{n,theo}$[a] (g/mol)	$M_{n,GPC}$[b] (g/mol)	PDI[b]
S1	60	2890	3300	1.10
S2	90	5920	6100	1.13
S3	120	7630	7900	1.15
S4	150	9670	9500	1.18
S5	180	11250	12200	1.22

[a] The theoretical number-average molecular weight was calculated according to the equation, $M_{n,theo} = M_M \times conv. \times [M]_0/[CTA]_0 + M_{CTA}$ where $M_{n,theo}$ is the theoretically calculated molecular weight of the polymer, M_M is the molecular weight of the monomer, conv is monomer conversion as determined by ^{1}HNMR spectroscopy, $[M]_0$ and $[CTA]_0$ the concentration of the monomer and the concentration of the RAFT agent, M_{CTA} is the molecular weight of the RAFT agent. [b] The number-average molecular weight (M_n) and molecular weight distribution (PDI=M_w/M_n) were measured by gel permeation chromatograph (GPC) on PS standards.

methyl groups on isopropyl.[35] At the same time, comparing to Figure 1b, the peak at 2100 cm^{-1} from $-N_3$ disappeared, which suggested the formation of the SiO_2-*g*-PNIPAM. The disappearance of the azide stretch after the click coupling indicates that most of the azides have been consumed during this reaction, although the low intensity of this IR absorption makes quantitation of conversion difficult.

To further confirm the covalent linkage mode and eliminate the possibility of physical absorption of alkyne-terminated poly(N-isopropylacrylamide) on the silica nanoparticle surface, we carried out a control experiment. We tried this coupling reaction with alkyne-terminated PNIPAM and azide-modified silica particles under the same conditions, but without the click reaction catalyst ($CuSO_4$/Na ascorbate). The silica nanoparticles obtained from this experiment showed the same FTIR spectrum as SiO_2-N_3 except that they lacked the absorption peaks of PNIPAM. This control confirms that the click reaction did not occur without the addition of catalyst. Noncovalent adsorption on the silica nanoparticle surface can thus be excluded as a possibility.

3.2. ^{1}H NMR Analysis. A carboxyl-terminated trithiocarbonate RAFT CTA was prepared by a previously reported one-step procedure.[31] This CTA is readily used to obtain carboxyl functionalized polymer. For the application of this type of CTA in click chemistry, we converted the terminal carboxyl group of CTA to an alkyne group via esterification with propargyl alcohol. The esterification reaction was done in the presence of EDC coupling agent and DMAP base. The ^{1}H NMR spectrum and peak assignments of alkyne-terminated RAFT CTA are presented in Figure 2a. ^{1}H NMR displayed the peaks at (a) 2.42 and (b) 4.66 ppm, which confirmed the attachment of propargyl group to CTA. The alkyne-terminated RAFT CTA was used in the synthesis of PNIPAM homopolymer. Figure 2b is the ^{1}H NMR spectrum of alkyne-terminated PNIPAM. On the spectrum, characteristic signals of PNIPAM at (j) 3.98 and (k) 1.12 ppm representing methyne and methyl protons on isopropyl groups were observed, which verified the successful synthesis of alkyne-terminated poly(N-isopropylacrylamide) chains.

3.3. Kinetic Studies. In order to investigate the living/controlled property of the RAFT polymerization of polymer chains, the polymerization kinetic studies on the synthesis of linear

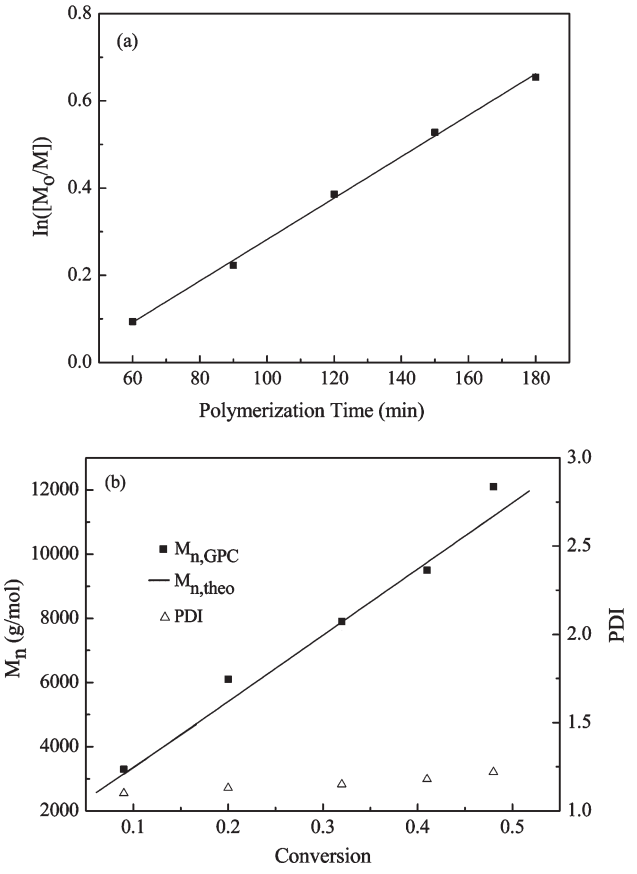

Figure 3. (a) Dependence of $\ln([M]_0/[M])$ on polymerization time in the RAFT polymerization of NIPAM. (b) Dependence of molecular weights and molecular weight distributions on monomer conversion. (Experimental conditions: $[NIPAM]_0/[CTA]_0/[AIBN]_0 = 200/1/0.2$; $[NIPAM]_0 = 1.4$ M; in 1,4-dioxane at 70 °C. Molecular weights of the polymers were calibrated on PS standards.).

PNIPAM were conducted. Our goal was to prepare low molecular weight PNIPAM (M_n =3300−12200 g/mol) with a terminal alkyne group. Detailed information was listed in Table 1. The polymerization kinetic for NIPAM was shown in Figure 3. A linear increasing in monomer conversion with time was observed (Figure 3a), which indicated a well controlled RAFT process by using the RAFT agent. Figure 3b showed the evolution of the number-average molecular weight (M_n) and molecular weight distribution (PDI) values of the obtained PNIPAM on the conversion for the RAFT polymerization of NIPAM in 1,4-dioxane at 70 °C. The $M_{n,GPC}$ values of the polymers increased linearly with monomer conversion while keeping low PDI values (PDI ≤ 1.22). At the same time, the experimental molecular weights were close to their corresponding theoretical ones at low monomer conversion.

3.4. Surface Analysis by XPS. The chemical composition of the modified silica surfaces was determined by XPS measurements (Figure 4). Figure 4a shows the XPS wide scan spectrum of the bare silica nanoaprticles. The presence of the C1s signals was probably associated with the adsorption of carbon dioxide (CO_2) or the presence of a trace amount of carbonaceous contaminants on the surface of silica nanoaprticles,[36] and the signal was weak. By comparison with Figure 4a, it can be seen that, from Figure 4b, a new signal of N1s appears, which is also confirmed by the N1s core-level spectrum as shown in Figure 4c.

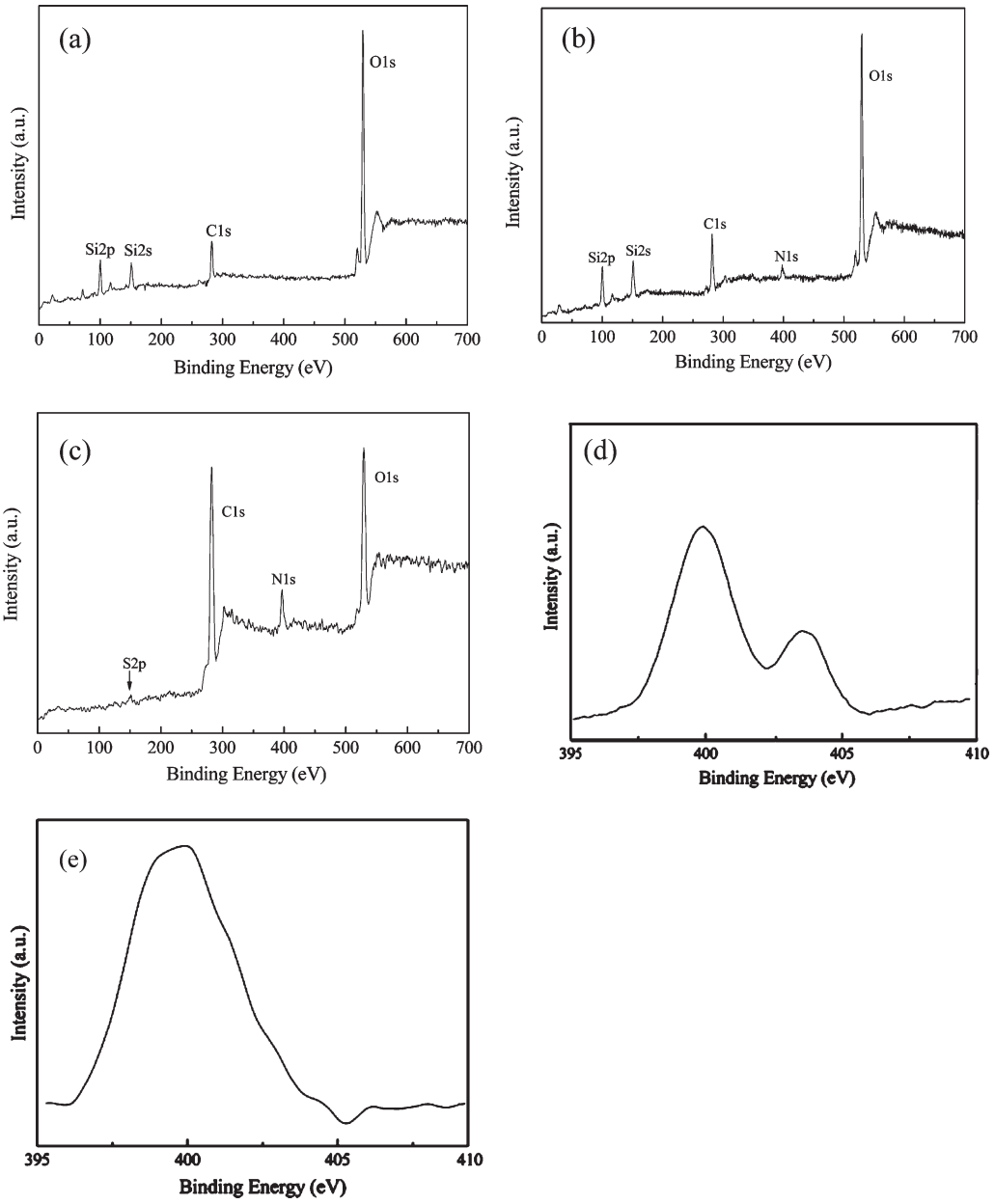

Figure 4. XPS (a) wide scan of the bare SiO_2, (b) wide scan of SiO_2-N_3, (c) wide scan of PNIPAM-functionalized SiO_2, (d) N1s core-level of SiO_2-N_3, and (e) N1s core-level of PNIPAM-functionalized SiO_2.

Compared to the XPS result of PNIPAM-grafted nanoparticles (Figure 4c) with that of SiO_2-N_3, the strong peak at the binding energy (BE) of 400.1 eV corresponding to N1s coming from the PNIPAAm shell and a new signal (161 eV) of S2p appeared besides the major peak at the BE of 532.8 eV ascribed to O1s and the peak at the BE of about 285.6 eV assigned to the C1s; moreover, the peak at the BE of 103.0 eV corresponding to Si2p and the peak at the BE of 154.7 eV corresponding to Si2s almost disappear (Figure 4b). The disappearance of the signals of silica indicates that whole the surfaces of the silica were coated by the PNIPAM with a thickness more than the detected depth (~8 nm for the organic matrix) for the XPS technique,[37] which is consistent with the thickness from the TEM results. Figure 4d presents high-resolution XPS spectra of the N1s region in the SiO_2-N_3 surfaces, and shows two peaks at 399.8 and 403.9 eV with an intensity ratio of 2:1, similar to other reports for azide groups on gold[33] and graphitic[38] surfaces. The high- and low-BE peaks are, respectively, assigned to the central, electron-deficient N atom in the azide group, and to the two nearly equivalent azide N atoms.[33] After the click reaction step, the N 1-s peak at 403.9 eV disappeared; the one at 400.1 eV becomes strong (Figure 4e), which can be taken as a clear evidence for a complete transformation of the azide group into the 1,2,3-triazole unit bound to the propargyl-terminated PNIPAM head. These changes for CuAAC functionalized surfaces were common to every situation we investigated, and are also consistent with literature observations.[39,40] It could be concluded that the PNIPAM chains had been grafted from the surfaces of silica nanoparticles.

3.5. TGA and EA Analysis. Figure 5 showed the TGA analysis of the bare SiO_2, SiO_2-N_3, and SiO_2-g-PNIPAM. The weight

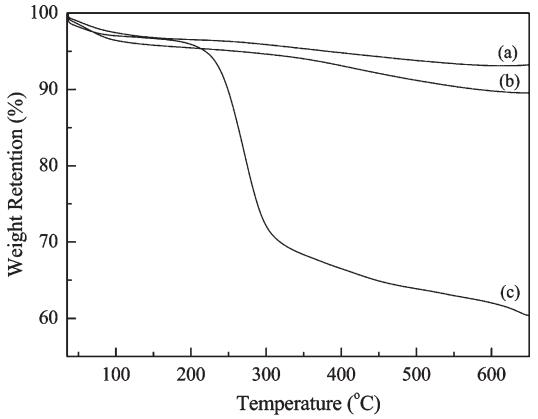

Figure 5. TGA curves obtained at a heating rate of 10 °C/min under a nitrogen atmosphere for (a) bare SiO_2, (b) azide-modified SiO_2, and (c) PNIPAM-functionalized SiO_2 having a polymer M_n = 12 200 g/mol.

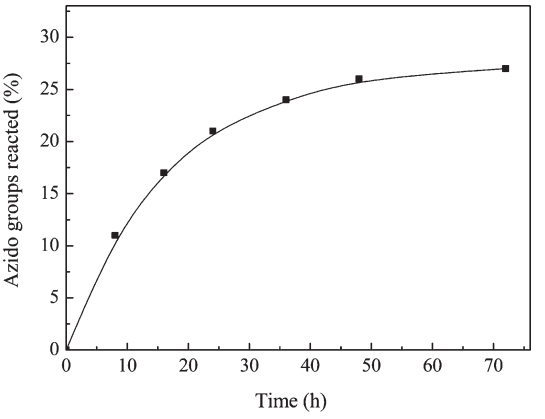

Figure 6. Kinetics of the click reactions of alkyne-PNIPAM to azide-modified SiO_2.

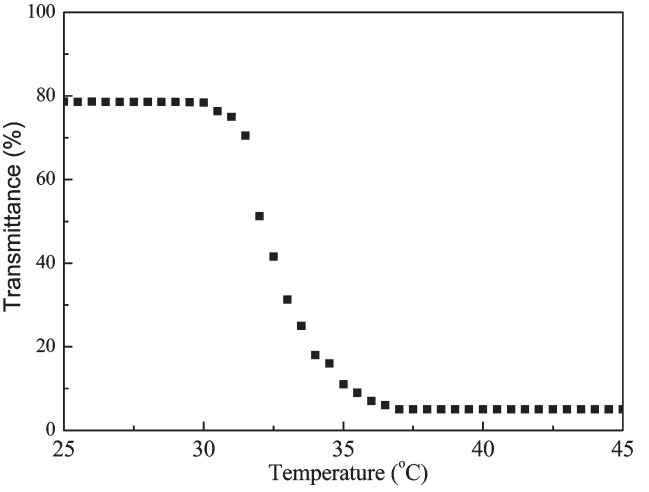

Figure 7. Transmittance changes of PNIPAM-functionalized SiO_2 aqueous solution with temperature.

loss below 200 °C, due to the physisorbed water and residual organic solvent, was 6.6% for bare silica (Figure 5a). We observed a weight loss of 4% (Figure 5b) for the azide-modified silica particles in the TGA curve. And the residual mass percentage was 91%. The surface grafting density of azide groups was calculated to be about 3.3 chains/nm^2 according to the eq 1. This is consistent with the result of 3.2 groups/nm^2 from the elemental analysis. Figure 5c showed the TGA curves of the click-modified silica particles with an azide-modified silica particles and low molecular weight PNIPAM with a terminal alkyne group. It showed that the weight loss percentage corresponding to the decomposition of PNIPAM chains was 36%. And the residual mass percentage was 57%. The surface grafting density of polymer was found to be about 0.62 chains/nm^2 calculated from eq 1, according to the TGA analysis. Using elemental analysis, the presence of PNIPAM on the surface of silica nanoparticle was confirmed.[41] Elemental analysis results were used to calculate the surface grafting density. We calculated that 0.64 PNIPAM chains were present on 1 nm^2 surface area of silica, which corresponds to a 1.41 nm distance between grafting sites according to eq 2. There have been few reports on the modification of silica nanoparticles by a RAFT polymer. Benicewicz and co-workers[42] deposited RAFT CTA on silica nanoparticles with grafting densities of 0.15−0.54 RAFT agents/nm^2. Guo and co-workers[43] immobilized a lactose-containing polymer onto silica gel particles with grafting densities 0.035−0.178 groups/nm^2. Tenhu and co-workers[44] employed the "grafting to" approach to prepare hybrid gold nanoparticles surface coated with PNIPAM brushes with a grafting density of 2.4 chains/nm^2, starting from thiol-terminated PNIPAM chains prepared via the RAFT process. In contrast, the surface grafting density obtained with an ATRP initiator was 2−5 groups/nm^2.[45] Comparing the grafting density of a RAFT CTA and ATRP initiator, lower grafting density is obtained with the RAFT CTA. This is likely due to the attachment of a more bulky RAFT CTA onto silica using the silanization reaction.[19] The grafting density of PNIPAM indicates that roughly 21% azide groups were converted during the click reaction with the alkyne-functionalized PNIPAM. This is in good agreement with the results of the TGA analysis (19%). TGA and EA also confirmed the presence of grafted polymer on the silica nanoparticle. The series of experiments in this work use quantitative EA to elucidate the kinetic trends that govern azide/alkyne cycloaddition on SiO_2 nanoparticle surfaces. The respective kinetic graph depicted in Figure 6 indicates that even at room temperature the rate of grafted polymers is relatively fast during the click reaction, with 20% of the available azido groups capturing substrate in less than 24 h. Saturation is essentially observed after 48 h, most probably due to the steric demands of the grafted polymers rendering the remaining azido groups inaccessible for further reaction.

3.6. Turbidity Measurements. It is well-known that thermo-responsive polymers can change their physical or chemical properties around the lower critical solution temperature (LCST). *N*-Isopropylacrylamide (NIPAM) is a water-soluble monomer whose polymer exhibits many fascinating properties.[46] It mimics the molecular structure of amino acids,[47] and its polymer exhibits a coil-to-globule transition at 32 °C (LCST). This property is the result of the rather complex polarity of this molecule. Below the LCST, the amide functionality imbibes water molecules, via hydrogen bonding, giving it both its water solubility and surface activity. However, moving above the transition temperature breaks these hydrogen bonds, and the polymer expels water molecules and undergoes a coil-to-globule transition, thereby precipitating to form particles. Owing to the thermosensitivity, PNIPAM has been widely investigated to fabricate thermosensitive micelles or gels for drug delivery

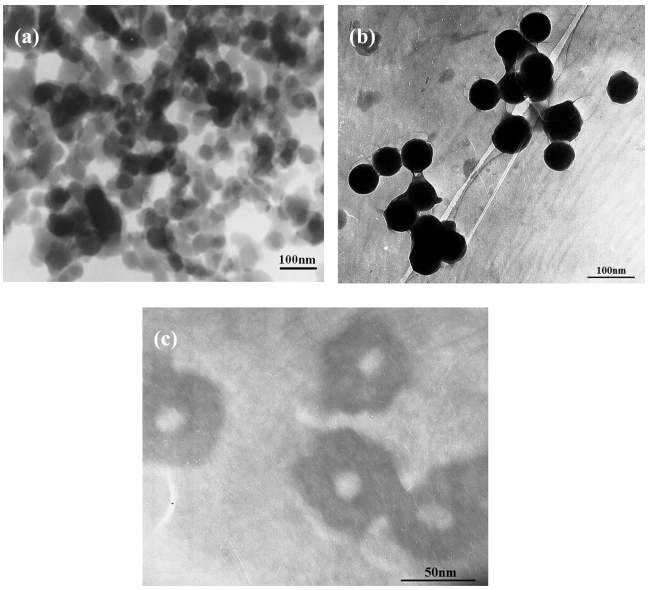

Figure 8. TEM images of (a) bare SiO_2 nanoparticles, (b) PNIPAM-functionalized SiO_2 nanoparticles, and (c) the temperature-responsive nanocapsules.

system.[48,49] UV−vis spectroscopy (λ = 500 nm) was used for transmission measurements on the aqueous solution of PNIPAM grafted hybrid silica nanoparticles with a concentration of 0.5 mg/mL. Transmission was monitored at temperature increment of 0.5 °C with equilibration time of 15 min. Figure 7 shows a plot of the transmittance versus temperature. The optical transmittance exhibits no changes in the range of 25−30 °C. In this temperature range, the outer zone of PNIPAM brushes still remain hydrophilic and the chains of polymers are extended and swelled in an aqueous solution. Above 30 °C, PNIPAM becomes hydrophobic and the chains of polymers are collapsed on the SiO_2 core and deswelled in aqueous solution, thus transmittance decreases abruptly from 78% to 6% in the temperature range 32−36 °C. By comparison with PNIPAM, our data for PNIPAM brushes on the exterior surface of SiO_2 nanoparticles show no sharp changes at any point throughout the transition. These observations are consistent with theoretical predictions that, as compared to the spherical surface, strong interchain interactions are present in the brush grafted to the substrate surface.[50] These enhanced interactions are thought to result in a broadening of the transition of polymer tethered on the substrate surface.[50]

3.7. TEM Analysis. The TEM images of the bare SiO_2 particles, the modified SiO_2 particles and the temperature-responsive nanocapsules were investigated using transmission electron microscopy to obtain information on size, shape, and distribution (Figure 8). The bare SiO_2 exhibited an average external diameter about 50 nm and showed large aggregates (Figure 8a). As can be seen in Figure 8b, after grafted with prepolymer based on NIPAM, the diameter of SiO_2-g-PNIPAM is larger than that of bare SiO_2 and SiO_2-g-PNIPAM shows spherical nanoparticles with roughened surfaces coated by polymers. The temperature-responsive nanocapsules were shown in Figure 8c, the TEM studies gave the direct evidence of the morphology of the nanocapsules. It can be seen from Figure 8c that the inner diameter of the nanocapsule was about 20 nm, which is smaller than the diameter of the primitive silica templates. It can be concluded that PNIPAM can successfully encapsulate grafted SiO_2 once SiO_2 particles are modified by click reaction.

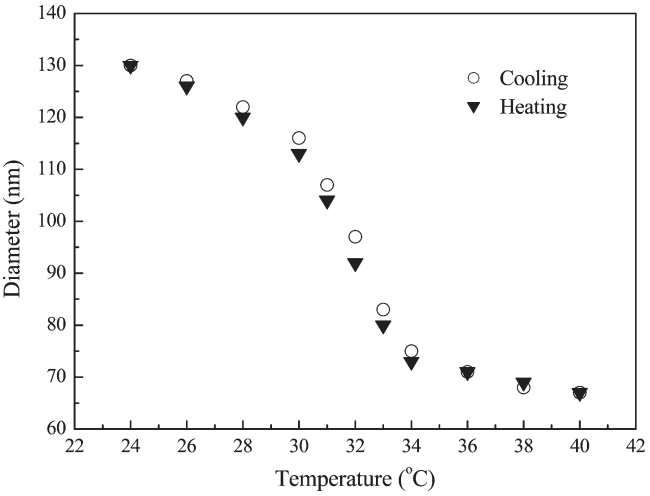

Figure 9. Kinetics of the smart shell on the surface of silica nanoparticles in response to change of temperature (5×10^{-3} mg/mL).

3.8. DLS Analysis. Dynamic light scattering (DLS) was employed to characterize temperature-dependent size changes of hybrid silica nanoparticles grafted with thermoresponsive PNIPAM brushes in aqueous solution (Figure 9). As expected, the diameter was decreased by the increase of temperature and increased by the decrease of temperature, and the change in the hydrodynamic diameters was reversible. At 24 °C, PNIPAM is hydrophilic and soluble in water; the hydrodynamic diameter of nanosphere is about 130 nm, and the PNIPAM chains are in a coil state, forming a solvated, incompact nanoshell on the exterior surface of SiO_2. The hydrodynamic diameter of the core−shell nanostructure decreased from 130 to 67 nm gradually with temperature increased from 24 to 40 °C, which resulted from the fact that the solubility of hydrophilic chains in water became more and more poor with increasing solution temperature and the fact that the long PNIPAM chains collapsed toward the surface of SiO_2, forming a compact closed nanoshell around the exterior surface of SiO_2. The hydrodynamic size of SiO_2-g-PNIPAM in water based on light scattering was much bigger than the diameter of SiO_2-g-PNIPAM obtained from TEM, which may have resulted from the fact that the PNIPAM chains and nanoparticles were solvated in water. Moreover, further DLS studies revealed that the swelling and collapse of PNIPAM brushes of hybrid silica nanoparticles were fully reversible upon cycling the solution temperature between 24 and 40 °C. In the DLS experiments, we did not observe the aggregation of nanoparticles at temperatures above the transition points, presumably because of the low concentrations.

4. CONCLUSIONS

In this study, we demonstrated a novel efficient postmodification route for preparation of smart hybrid SiO_2 nanoparticles with a stimuli-responsive nanoshell based on RAFT and click chemistry. This new route allows an easy control of molecular weight, molecular weight distributions, and architecture of grafted polymers onto solid surfaces. We also observed that, the grafting density of polymer chains can be easily adjusted by changing the react time. The as-synthesized hybrid SiO_2

nanoparticles with a thermo-responsive nanoshell were determined by FTIR, XPS, TGA, TEM, DLS and UV−vis. The smart nanoshell undergoes reversible switches between solvated, incompact open nanoshell and compact closed nanoshell upon changing the temperature of the solution, and this new core−shell nanomaterial will have potential applications in controlled release of drug, DNA, protein, the smart catalyst, smart separation system, and preparation of smart nanoreactors.

AUTHOR INFORMATION

Corresponding Author

*Tel.: +86 931 8912387. Fax: +86 931 8912582. E-mail: mzliu@lzu.edu.cn (M.Z. Liu).

ACKNOWLEDGMENT

The financial support of the Special Doctorial Program Funds of the Education of China (Grant 20090211110004) and Gansu Province Project of Science and Technologies (Grant 0804WCGA130) is gratefully acknowledged.

REFERENCES

(1) Okamoto, M. *Mater. Sci. Technol.* **2006**, *22*, 756.
(2) Koleva, D. A.; Boshkov, N.; Bachvarov, V.; Zhan, H.; Breugel, K. *Surf. Coat. Technol.* **2010**, *204*, 3760.
(3) Ver Meer, M. A.; Narasimhan, B.; Shanks, B. H.; Mallapragada, S. K. *ACS Appl. Mater. Interfaces* **2010**, *2*, 41.
(4) Lee, J. Y.; Lee, H. K. *Mater. Chem. Phys.* **2004**, *85*, 410.
(5) Zhu, M. Q.; Wang, L. Q.; Exarhos, G. J.; Li, A. D. Q. *J. Am. Chem. Soc.* **2004**, *126*, 2656.
(6) Wu, T.; Zhang, Y. F.; Wang, X. F.; Liu, S. Y. *Chem. Mater.* **2008**, *20*, 101.
(7) Hong, C. Y.; Li, X.; Pan, C. Y. *J. Phys. Chem. C* **2008**, *112*, 15320.
(8) Dong, J. K.; Sung, M. K.; Bokyung, K.; Wan-Joong, K.; Hyun-jong, P.; Hyeon, C.; Insung, S. C. *Macromol. Chem. Phys.* **2005**, *206*, 1941.
(9) Li, H. M.; Cheng, F. Y.; Duft, A. M.; Adronov, A. *J. Am, Chen. Soc.* **2005**, *127*, 14518.
(10) Drockenmuller, E.; Colinet, I.; Damiron, D.; Gal, F.; Perez, H.; Carrot, G. *Macromolecules* **2010**, *43*, 9371.
(11) Kolb, H. C.; Finn, M. G.; Sharpless, K. B. *Angew. Chem., Int. Ed.* **2001**, *40*, 2004.
(12) Li, G. L.; Wan, D.; Neoh, K. G.; Kang, E. T. *Macromolecules* **2010**, *43*, 10275.
(13) Li, B. L.; Liu, Z. T.; He, Y. M.; Pan, J.; Fan, Q. H. *Polymer* **2008**, *49*, 1527.
(14) Samia, M. C.; Sarra, G. D.; Claire, M.; Mohamed, M. C. *Chem. Soc. Rev.* **2011**, *40*, 4143.
(15) Samia, M. C.; Alexandre, L.; Fayna, M.; Frédéric, H; Benjamin, C.; Hatem, B. R.; Michel, D; Mohamed, M. C. *Langmuir* **2010**, *26*, 16115.
(16) Feng, X. S.; Taton, D.; Ibarboure, E.; Chaikof, E. L.; Gnanou, Y. *J. Am. Chem. Soc.* **2008**, *130*, 11662.
(17) Kacprzak, K. M.; Maier, N. M.; Lindner, W. *Tetrahedron Lett.* **2006**, *47*, 8721.
(18) Ranjan, R.; Brittain, W. J. *Macromolecules* **2007**, *40*, 6217.
(19) Zhang, T.; Wu, Y. P.; Pan, X. M.; Zheng, Z. H.; Ding, X. B.; Peng, Y. X. *Eur. Polym. J.* **2009**, *45*, 1625.
(20) Chiefari, J.; Chong, Y. K.; Ercole, F.; Krstina, J.; Jeffery, J.; Le, T. P. T.; Mayadunne, R. T. A.; Meijs, G. F.; Moad, C. L.; Moad, G.; Rizzardo, E.; Thang, S. *Macromolecules* **1998**, *31*, 5559.
(21) Wang, L. P.; Wang, Y. P.; Wang, R. M.; Zhang, S. C. *React. Funct. Polym.* **2008**, *68*, 643.
(22) Lian, X. M.; Wu, D. X.; Song, X. H.; Zhao, H. Y. *Macromolecules* **2010**, *43*, 7434.
(23) De, P.; Gondi, S. R.; Sumerlin, B. S. *Biomacromolecules* **2008**, *9*, 1064.
(24) Pei, X. W.; Hao, J. C.; Liu, W. M. *J. Phys. Chem. C* **2007**, *111*, 2947.
(25) Feng, X. S.; Taton, D.; Borsali, R.; Chaikof, E. L.; Gnanou, Y. *J. Am. Chem. Soc.* **2006**, *128*, 11551.
(26) Moustafine, R. I.; Salachova, A. R.; Frolova, E. S.; Kemenova, V. A.; Van den Mooter, G. *Drug Dev. Ind. Pharm.* **2009**, *35*, 1439.
(27) Moustafine, R. I.; Bobyleva, V. L.; Bukhovets, A. V.; Garipova, V. R.; Kabanova, T. V.; Kemenova, V. A.; Van den Mooter, G. *J. Pharm. Sci.* **2011**, *100*, 874.
(28) Rafael, C. C.; Jessica, P.; Isabel, P. S.; Jorge, P. J.; Antonio, F. B.; Luis, M. L. M. *Adv. Funct. Mater.* **2009**, *19*, 3070.
(29) Schild, H. G. *Prog. Polym. Sci.* **1992**, *17*, 163.
(30) Voronov, A.; Shafranska, O. *Langmuir* **2002**, *18*, 4471.
(31) Lai, J. T.; Filla, D.; Shea, R. *Macromolecules* **2002**, *35*, 6754.
(32) Hudalla, G. A.; Murphy, W. L. *Langmuir* **2009**, *25*, 5737.
(33) Collman, J. P.; Devaraj, N. K.; Eberspacher, T. P. A.; Chidsey, C. E. D. *Langmuir* **2006**, *22*, 2457.
(34) Thode, C. J.; Williams, M. E. *J. Colloid Interface Sci.* **2008**, *320*, 346.
(35) Pan, Y. V.; Wesley, R. A.; Luginbuhl, R.; Denton, D. D.; Ratner, B. D. *Biomacromolecules* **2001**, *2*, 32.
(36) Kurokawa, Y.; Hirose, H.; Moriya, T.; Kimura, C. *Jpn. J. Appl. Phys.* **1999**, *38*, 5040.
(37) Briggs, D. *Surface Analysis of Polymers by XPS and Static SIMS*; Cambridge University Press: New York, 1998.
(38) Marrani, A. G.; Dalchiele, E. A.; Zanoni, R.; Decker, F.; Cattaruzza, F.; Bonifazi, D.; Prato, M. *Electrochim. Acta* **2008**, *53*, 3903.
(39) Devadoss, A.; Chidsey, C. E. D. *J. Am. Chem. Soc.* **2007**, *129*, 5370.
(40) Collman, J. P.; Devaraj, N. K.; Chidsey, C. E. D. *Langmuir* **2004**, *20*, 1051.
(41) Bartolome, C.; Beyou, E.; Chaumont, P.; Zydowicz, N. *Macromolecules* **2003**, *36*, 7946.
(42) Li, C.; Han, J.; Ryu, C. Y.; Benicewicz, B. C. *Macromolecules* **2006**, *39*, 3175.
(43) Guo, T. Y.; Liu, P.; Zhu, J. W.; Song, M. D.; Zhang, B. H. *Biomacromolecules* **2006**, *7*, 1196.
(44) Shan, J.; Chen, J.; Nuopponen, M.; Tenhu, H. *Langmuir* **2004**, *20*, 4671.
(45) von Werne, T.; Patten, T. E. *J. Am. Chem. Soc.* **2001**, *123*, 7497.
(46) Pelton, R. *Adv. Colloid Interface Sci.* **2000**, *85*, 1.
(47) Tiktopulo, E. I.; Uversky, V. N.; Lushchik, V. B.; Klenin, S. I.; Bychkova, V. E.; Ptitsyn, O. B. *Macromolecules* **1995**, *28*, 7519.
(48) Liu, Y. Y.; Shao, Y. H.; Lv, J. *Biomaterials* **2006**, *27*, 4016.
(49) Nakayama, M.; Chung, J. E.; Miyazaki, T.; Yokoyama, M.; Sakai, K.; Okano, T. *React. Funct. Polym.* **2007**, *67*, 1398.
(50) Balamurugan, S.; Mendez, S.; Balamurugan, S. S.; O'Brien, M. J.; Lopez, G. P. *Langmuir* **2003**, *19*, 2545.